NJC

New Journal of Chemistry

A journal for new directions in chemistry

Accepted Manuscript

This article can be cited before page numbers have been issued, to do this please use: X. Shu, Y. Fan, S. Li, Y. Jin, C. Xia and C. Huang, *New J. Chem.*, 2020, DOI: 10.1039/C9NJ05785D.

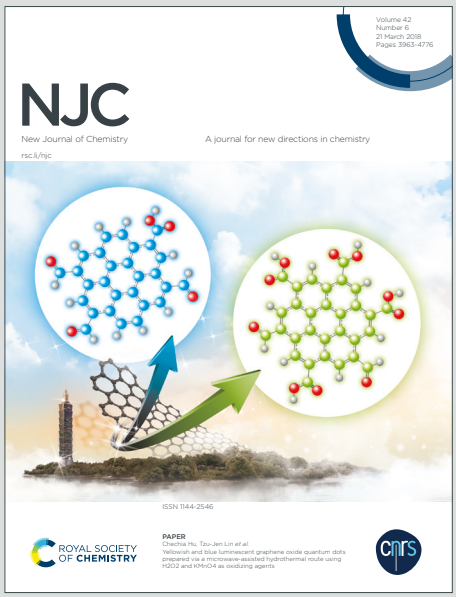

This is an Accepted Manuscript, which has been through the Royal Society of Chemistry peer review process and has been accepted for publication.

Accepted Manuscripts are published online shortly after acceptance, before technical editing, formatting and proof reading. Using this free service, authors can make their results available to the community, in citable form, before we publish the edited article. We will replace this Accepted Manuscript with the edited and formatted Advance Article as soon as it is available.

You can find more information about Accepted Manuscripts in the Information for Authors.

Please note that technical editing may introduce minor changes to the text and/or graphics, which may alter content. The journal's standard Terms & Conditions and the Ethical guidelines still apply. In no event shall the Royal Society of Chemistry be held responsible for any errors or omissions in this Accepted Manuscript or any consequences arising from the use of any information it contains.

Anion binding and fluoride ion induced conformational changes in bisurea receptors

Xi Shu, Yu Fan, Shoujian Li, Yongdong Jin, Chuanqin Xia and Chao Huang*

College of Chemistry, Sichuan University, No.29 Wangjiang Road, Chengdu 610064, Sichuan, PR China.

*E-mail: chuang@scu.edu.cn

Abstract

Two types of bisurea receptors, containing either 2,6-substituted phenyl or 2,6-substituted pyridine, are prepared, and their anion binding properties are investigated. Compared with the phenyl bisurea receptors, the pyridine bisurea receptors can be more easily converted to a *cis-cis* conformation from a *trans-trans* conformation, providing a cavity that more closely matches the volume of a fluoride ion and increasing the number of NH sites bound to the fluoride ion. As a result, the pyridine bisurea in *cis-cis* conformation shows stronger affinity and higher selectivity to fluoride ions, which is supported by crystal structure analysis and NMR titration experiments. Through DFT calculations, a mechanism of fluoride ion induced conformational changes of pyridine bisurea receptors is proposed, and the energy barriers of conformational changes for both types of receptors are determined.

Keywords: bisurea receptors; anion recognition; crystal structure; NMR titration;

View Article Online
DOI: 10.1039/C9NJ05785D

Introduction

Anions play indispensable roles in catalysis, environmental science, and biological systems, including in medicine.[1-7] Typically, F^- ions are widely present in soil, groundwater, and the ocean at concentrations of $10^1 - 10^2$ μM.[8] Long-term intake of excess fluoride (>1.5 mg L^{-1})[9] is a serious hazard to human health, resulting in dental and bone fluorosis or neurological damage.[10] Anion receptors can identify, detect, and remove anions (such as fluoride ions) in the environment to prevent excessive amounts of anions from harming people. In recent years, many urea-based receptors for anion recognition have been developed.[11-13] Specifically, a series of highly efficient urea receptors were designed by attaching urea groups to calixarenes[14-18], ferrocene[19,20], triethylamine[21,22], macrocyclic compounds[23-26], crown ethers[27,28], oxazoles[29] and oximes[30,31]. In most of these, the urea groups are present in a *cis* conformation.[32] From crystal structure analysis of urea compounds, in general, the urea groups exist in two stable conformations, *cis* and *trans*, as shown in Scheme 1.[33-37] It is well known that conversions in conformation are very important.[38] For example, the properties of nano-dimensional assemblies[38], surfaces[39], and biological molecules[40] can be affected by conformational transitions. Therefore, it is necessary to determine the factors and mechanisms that influence conformational changes for anion receptors.[41] The main factors causing conformational changes are hydrogen bonding[42-45], van der Waals forces[46], dipole-dipole interactions[47].

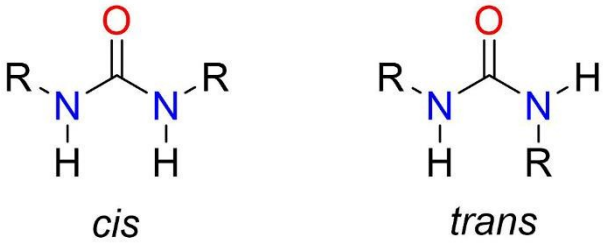

Scheme 1. The *cis* and *trans* conformations of a urea group.

Recently, interesting crystal structures of novel urea-based receptors were measured[48,49] in which the urea groups all exhibited the *cis* conformation, the same as most of the reported urea receptor structures listed above.[14-31] However, the urea group of pyridine bisurea receptors showed a *trans* conformation. This is due to hydrogen bonding between the carbonyl group of the pyridine and one of the N–H groups of the urea, which leads to the formation of a six-membered ring, favoring the trans-trans conformation across the molecule (Scheme 2). However, when a F^- ion is added, it

disrupts the intramolecular hydrogen bonds, causing the OC–NH single bond to rotate and inducing a transition of the receptor from *trans-trans* to *cis-cis*. To the best of our knowledge, fluoride ion induced transition of a urea conformation from *trans* to *cis* has not been reported previously. It should be noted that there are only a few examples of conformational transition in general of urea-based receptors in the *cis* conformation. For example, Gale et al. found that CH_3COO^- can cause an N–C single bond rotation between a urea and phenyl group in 1, 3-diindolylureas.[50] Makuc et al. found that CH_3COO^- can also induce conformational changes of indole functionalized urea receptors.[51] Yamato et al. have proposed that F^- ions cause a conformation change in thiacalix[4]arene receptors, specifically, that the intramolecular hydrogen bonds between the two adjacent urea groups in one receptor were destroyed.[52] However, these studies did not provide crystal structures to illustrate the absolute conformational changes of urea receptors.

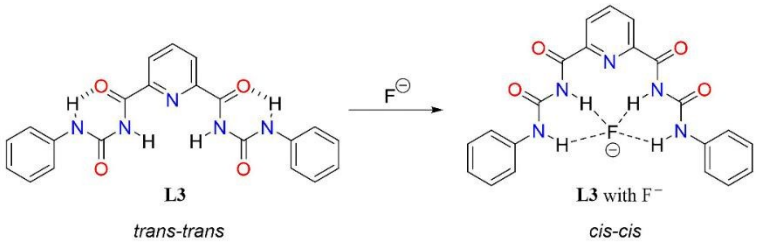

Scheme 2. Fluoride ion induced conformational conversion of the bisurea **L3** from a *trans-trans* conformation to a *cis-cis* conformation.

In this paper, the synthesis and characterization of a series of pyridine bisurea receptors is described (**L1-L3** in Scheme 3). The conformational stability of these urea receptors and their interactions with anions are systematically investigated through crystal structure analysis, NMR titration, and theoretical calculations. In order to further understand the influence of the pyridine ring on conformational stability and transition of urea group, phenyl bisurea receptors were also synthesized (**L4-L5** in Scheme 3). The structures and anion binding properties of **L4** and **L5** are compared with the pyridine bisurea receptors.

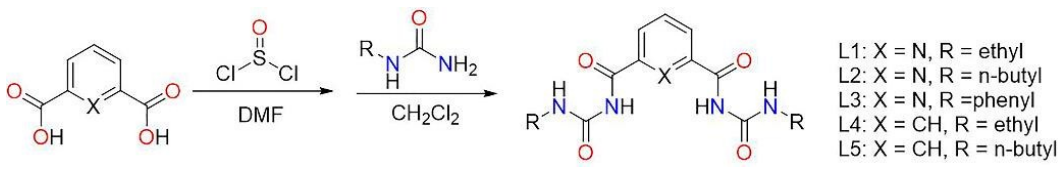

Scheme 3. Synthetic route for the receptors **L1-L5**

View Article Online
DOI: 10.1039/C9NJ05785D

Experimental

Materials and general methods

Unless otherwise stated, chemical reagents were obtained from commercial suppliers and used without further purification. All solvents used were purified and dried by standard methods prior to use. ^{1}H NMR (400 MHz) and ^{13}C NMR (100 MHz) spectra were recorded on a Bruker AV III 400 MHz spectrometer with either DMSO-d_6 or $CDCl_3$ as the solvent, and tetramethylsilane (TMS) as an internal reference. High resolution mass spectrometry (HRMS) was carried out on a Shimadzu LCMS-IT-TOF (ESI) spectrometer.

Synthesis

L1-L2 were prepared following a procedure identical to one previously reported in the literature.[53] **L3-L5** were prepared following a similar procedure as **L1-L2**, described as follows:

A mixture of pyridine-2, 6-dicarboxylic acid or isophthalic acid (10 mmol), $SOCl_2$ (10 mL) and DMF (0.2 mL) was refluxed for 5 h under a nitrogen atmosphere. Excess $SOCl_2$ was removed by reduced pressure distillation, and the mixture was further cooled in an ice bath. 50 mL of a solution of ethylurea, n-butylurea, or phenylurea (22 mmol) in CH_2Cl_2 was then added dropwise. The mixture was stirred overnight at room temperature. Solvents were removed from the reaction mixture, and the resulting material was washed alternately with diethyl ether and water by vigorous stirring to obtain a white solid.

L1: 1.51 g, yield 49%. Melting point: 193-196 °C. ^{1}H NMR (400 MHz, $CDCl_3$) δ = 10.76 (s, 2H, H_a), 8.49 (t, 2H, J = 5.3 Hz, H_b), 8.44 (d, 2H, J = 7.9 Hz, H_c), 8.16 (t, 1H, J = 7.4 Hz, H_d), 3.41 (dq, 4H, J = 7.2 Hz, H_e), 1.24 (t, 6H, J = 7.3 Hz, H_f).

L2: 2.44 g, yield 67%. Melting point: 187-190 °C. ^{1}H NMR (400 MHz, $CDCl_3$) δ = 10.77 (s, 2H, H_a), 8.58 (t, 2H, J = 5.7 Hz, H_b), 8.44 (d, 2H, J = 7.8 Hz, H_c), 8.14 (t, 1H, J = 7.8 Hz, H_d), 3.34 (dt, 4H, J = 6.9 Hz, J = 5.7 Hz, H_e), 1.42, 1.57 (two multiplets, 8H, $H_{g,f}$), 0.92 (t, 6H, J = 7.2 Hz, H_h).

L3: 2.72 g, yield 68%. Melting point: 231-234 °C. ^{1}H NMR (400 MHz, $CDCl_3$) δ 10.98 (s, 2H, H_a), 10.56 (s, 2H, H_b), 8.55 (d, 2H, *J* = 7.8 Hz, H_c), 8.24 (t, 1H, *J* = 7.8 Hz, H_d), 7.46 (d, 4H, *J* = 7.9 Hz, H_e), 7.27 (t, 4H, *J* = 7.3 Hz, H_f), 7.10 (t, 2H, *J* = 7.4 Hz, H_g). ^{13}C NMR (101 MHz, $CDCl_3$) δ = 164.25, 151.04, 147.59, 139.85, 137.00, 128.89, 127.20, 124.50, 120.72. HRMS (ESI^+): calcd for $C_{22}H_{20}N_2O_8Na^+$ $[M+Na]^+$ 426.1173; found 426.1168.

L4: 1.43 g, yield 47%. Melting point: 213-217 °C. ^{1}H NMR: ^{1}H NMR (400 MHz, $CDCl_3$) δ = 9.47 (s, 2H, H_a), 8.59 (t, 2H, *J* = 5.7 Hz, H_b), 8.47 (s, 1H, H_c), 8.15 (d, 2H, *J* = 7.8 Hz, H_d), 7.65 (t, 1H, *J* = 7.8 Hz, H_e), 3.38 (dq, 4H, *J* = 7.2 Hz, H_f), 1.21 (t, 6H, *J* = 7.3 Hz, H_g). ^{13}C NMR (101 MHz, DMSO-*d*$_6$) δ = 167.71, 153.56, 133.17, 132.62, 129.57, 127.98, 34.50, 15.42. HRMS (ESI^+): calcd for $C_{14}H_{18}N_4O_4Na^+$ $[M+Na]^+$ 329.1220; found 329.1182.

L5: 1.98 g, yield 54%. Melting point: 204-208 °C. ^{1}H NMR (400 MHz, $CDCl_3$) δ = 10.19 (s, 2H, H_a), 8.71 (t, 2H, *J* = 5.7 Hz, H_b), 8.56 (s, 1H, H_c), 8.23 (d, 2H, *J* = 7.8 Hz, H_d), 7.63 (t, 1H, *J* = 7.8 Hz, H_e), 3.32 (td, 4H, *J* = 7.0 Hz, *J* = 5.6 Hz, H_f), 1.53 (p, 4H, *J* = 7.1 Hz, H_g), 1.36 (m, 4H, H_h), 0.91 (t, 6H, *J* = 7.3 Hz, H_i). ^{13}C NMR (101 MHz, $CDCl_3$) δ = 167.50, 154.43, 132.95, 132.62, 129.30, 127.35, 39.62, 31.48, 20.08, 13.71. HRMS (ESI^+): calcd for $C_{18}H_{26}N_4O_4Na^+$ $[M+Na]^+$ 385.1846; found 385.1805.

NMR titration

^{1}H NMR titration measurements were conducted in either $CDCl_3$ or DMSO-*d*$_6$, in both cases at room temperature. ^{19}F NMR titration measurements were conducted in DMSO-*d*$_6$ at room temperature.

In the case of $CDCl_3$, the initial concentration of receptors **L3** and **L4** was 5×10^{-3} M. 0.05 M stock solutions of the anions (F^-, Cl^-, Br^-, I^-, NO_3^-, PF_6^-, CH_3COO^-, ClO_4^-, HSO_4^-, $H_2PO_4^-$ or ReO_4^-, as tetrabutylammonium, TBA, salts) were prepared by dissolving the salt in $CDCl_3$ solution. NMR samples were then prepared by adding the anion solution (50 μL) to 500 μL of the receptor solution.

For DMSO-*d*$_6$ solutions, the initial concentration of receptors **L3** and **L4** was 2.0×10^{-3} M. Stock solutions of the anion, Cl, Br, H_2PO_4 and CH_3COO as TBA salts, were 0.4 M in DMSO-*d*$_6$ solution. NMR samples were prepared by adding varying amounts of the anion solutions (0–25 μL) to 500 μL of the receptor solution.

View Article Online
DOI: 10.1039/C9NJ05785D

X-ray crystallography

Crystals suitable for X-ray diffraction (XRD) were obtained for **L1**, **L3** and **L5**. Single crystal XRD data for these materials were collected on an Agilent Gemini, Dual, Cu at zero, EosS2 diffractometer equipped with a graphite-monochromated Cu Kα (λ = 0.154184 nm) source. The intensity data was collected by the u scan technique. Using Olex2, the structure was solved with the ShelXT structure solution program using Direct Methods and refined with the ShelXL refinement package by least-squares minimization.[54-56] X-ray crystallographic information data (CIFs) is available in the Cambridge Crystallographic Data Centre under numbers 1536295 (**L1**), 1944338 (**L1**·H_2O), 1944331 (**L3**), 1944326 (**L3**·TBAF), and 1944332 (**L5**).

Crystal Data for $C_{26}H_{34}N_{10}O_8$ (**L1**) (*M* = 614.63 g/mol): triclinic, space group P-1 (no. 2), *a* = 9.0672(4) Å, *b* = 13.1124(7) Å, *c* = 14.5279(7) Å, *α* = 92.323(4)°, *β* = 106.840(4)°, *γ* = 110.178(5)°, *V* = 1532.64(14) Å^3, *Z* = 2, *T* = 293.52(10) K, μ(CuKα) = 0.851 mm^{-1}, *Dcalc* = 1.332 g/cm^3, 13339 reflections measured (10.678° ≤ 2Θ ≤ 144.85°), 5849 unique (R_{int} = 0.0446, R_{sigma} = 0.0446) which were used in all calculations. The final R_1 was 0.0835 (I > 2σ(I)) and wR_2 was 0.2226 (all data).

Crystal Data for $C_{13}H_{19}N_5O_5$ (**L1**·H_2O) (*M* =325.33 g/mol): monoclinic, space group P21/c (no. 14), *a* = 7.9330(3) Å, *b* = 21.6567(7) Å, *c* = 9.2173(3) Å, *β* = 105.934(4)°, *V* = 1522.70(9) Å^3, *Z* = 4, *T* = 294.33(10) K, μ(CuKα) = 0.937 mm^{-1}, *Dcalc* = 1.419 g/cm^3, 8364 reflections measured (10.786° ≤ 2Θ ≤ 144.906°), 2967 unique (R_{int} = 0.0307, R_{sigma} = 0.0289) which were used in all calculations. The final R_1 was 0.0529 (I > 2σ(I)) and wR_2 was 0.1405 (all data).

Crystal Data for $C_{42}H_{34}N_{10}O_8$ (**L3**) (*M* =806.79 g/mol): triclinic, space group P-1 (no. 2), *a* = 10.0589(9) Å, *b* = 12.8100(9) Å, *c* = 15.9508(13) Å, *α* = 77.077(7)°, *β* = 87.942(7)°, *γ* = 78.291(7)°, *V* = 1961.5(3) Å^3, *Z* = 2, *T* = 295.0(3) K, μ(CuKα) = 0.812 mm^{-1}, *Dcalc* = 1.366 g/cm^3, 21475 reflections measured (8.978° ≤ 2Θ ≤ 147.772°), 7653 unique (R_{int} = 0.0728, R_{sigma} = 0.0743) which were used in all calculations. The final R_1 was 0.0797 (I > 2σ(I)) and wR_2 was 0.2301 (all data).

Crystal Data for $C_{37}H_{53}FN_6O_4$ (**L3**·TBAF) (*M* =664.85 g/mol): monoclinic, space group P21/n (no. 14), *a* = 12.2710(3) Å, *b* = 17.4802(4) Å, *c* = 19.5368(4) Å, *β* =

107.634(3)°, V = 3993.72(16) Å^3, Z = 4, T = 296.31(10) K, μ(CuKα) = 0.612 mm^{-1}, *Dcalc* = 1.106 g/cm^3, 22804 reflections measured (9.098° ≤ 2Θ ≤ 145.65°), 7792 unique (R_{int} = 0.0342, R_{sigma} = 0.0278) which were used in all calculations. The final R_1 was 0.0641 (I > 2σ(I)) and wR_2 was 0.2042 (all data).

Crystal Data for $C_{18}H_{26}N_4O_4$ (**L5**) (M =362.43 g/mol): monoclinic, space group C2/c (no. 15), a = 16.8164(6) Å, b = 12.1616(4) Å, c = 9.6474(3) Å, β = 98.674(3)°, V = 1950.46(12) Å^3, Z = 4, T = 295.39(10) K, μ(CuKα) = 0.727 mm^{-1}, *Dcalc* = 1.234 g/cm^3, 5510 reflections measured (10.644° ≤ 2Θ ≤ 145.206°), 1895 unique (R_{int} = 0.0226, R_{sigma} = 0.0190) which were used in all calculations. The final R_1 was 0.0766 (I > 2σ(I)) and wR_2 was 0.1810 (all data).

Theoretical studies

All calculations were performed using Gaussian 09.[57] Geometries were optimized using the M06-2X functional[58] with the basis set 6-311G (d, p) for all atoms. Frequency computations were performed at the same theoretical levels to ensure that the determined structures correspond to a local minimum on the potential energy surface. The single point energy was calculated according to the M06-2X/ def2-TZVP[59] level for the optimized geometry. 3D molecular structures of all species shown here were drawn with the CYL view program.[60]

View Article Online
DOI: 10.1039/C9NJ05785D

Results and discussion

As shown in Scheme 3, receptors **L1** through **L5** were synthesized using similar methods. Briefly, pyridine-2,6-dicarboxylic acid or isophthalic acid is reacted with thionyl chloride under nitrogen to give an acid chloride, which is reacted with urea derivatives to obtain the corresponding crude product. The crude product was washed with diethyl ether and water, respectively, to generate a white powdery solid (**L1-L5**, yield: 40–70%), which was characterized by ^{1}H-NMR, ^{13}C-NMR, HR-MS.

Crystal Structures

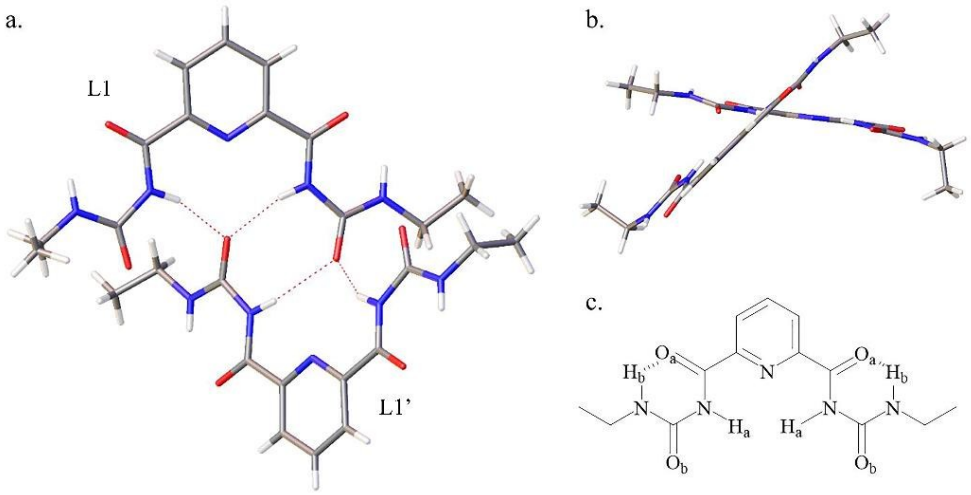

Figure 1. (a, b) Two views of the crystal structure of **L1**; (c) chemical structure of **L1**. (C: gray, H: white, O: red, N: blue)

As shown in Figure 1a, **L1** adopts a dimer form. The C=O_b of one receptor molecule forms two intermolecular hydrogen bonds with N–H_a groups of another receptor (N–H_a⋯O_b: 2.200, 2.237 Å). Meanwhile, C=O_b of the second receptor molecule and two N–H_a groups of the first also form intermolecular hydrogen bonds with length 2.232 and 2.342 Å. In addition, the two urea groups of each receptor molecule have a *trans-trans* conformation, like the *trans-trans* conformation in Scheme 2. The two distal N–H_b of the urea groups form intramolecular hydrogen bonds with the C=O_a (C=O_a⋯H_b–N:**L1**, 2.002, 2.013 Å; **L1'**, 2.043, 2.053 Å), constituting two stable six-membered ring structures. The pyridine N_{Py} atom forms two intramolecular hydrogen bonds with the N–H_a of the two urea groups (**L1**: 2.273, 2.271 Å; **L1'**: 2.283, 2.304 Å).

As shown in Figure 1b, the two six-membered ring planes are almost coplanar with the plane of the pyridine ring. The dihedral angles between the six-membered ring and the pyridine ring are 9.98°(**L1**), -0.93°(**L1**) and 4.98°(**L1'**), 0.92° (**L1'**), respectively. Moreover, the two receptor molecules are stacked in a cross-structure manner (Figure 1b).

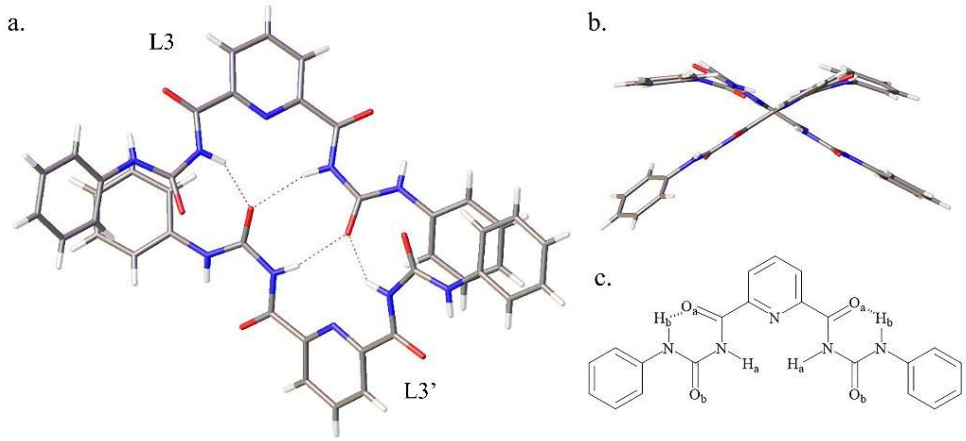

Figure 2. (a, b) Two views of the crystal structure of **L3** (c) chemical structure of **L3**. (C: gray, H: white, O: red, N: blue)

The crystal structure of **L2** has been reported elsewhere[53], and we have also obtained the crystal structure of **L3** (Figure 2). There are no significant differences in the molecular conformations of **L1**, **L2,** and **L3**, except for slight differences in the length of the hydrogen bonds and the dihedral angles.

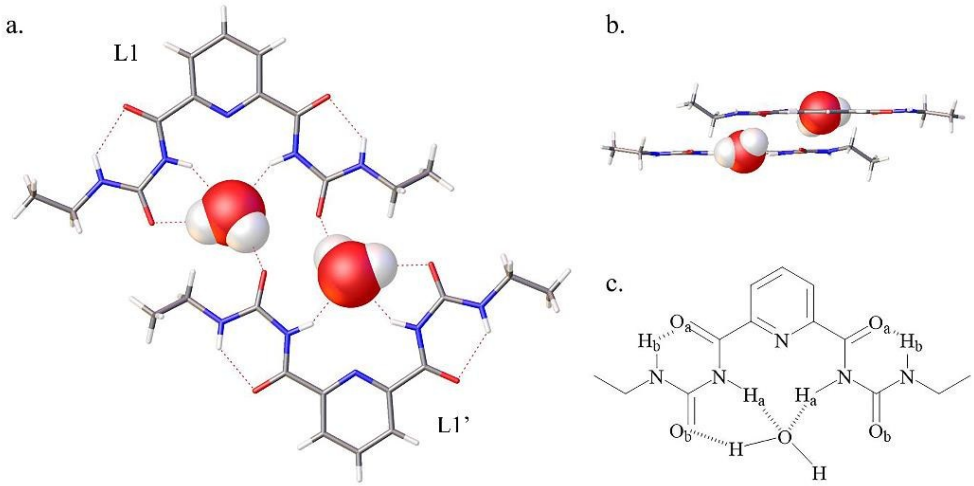

Figure 3. (a, b) Two views of the crystal structure of **L1·H₂O** (c) chemical structure of **L1·H₂O**. (C: gray, H: white, O: red, N: blue)

The crystal structure of the **L1**·H_2O complex is shown in Figure 3a. The two urea groups in the receptor molecule are still adopt a *trans-trans* conformation, and the two distal N–H_b of the urea groups form intramolecular hydrogen bonds with the carbonyl oxygen (C=O_a···H_b–N: 1.994, 2.072 Å), generating stable six-membered ring structures. The oxygen atom in water and two N–H_a on urea groups form N–H_a···O intermolecular hydrogen bonds (2.213 Å and 2.216 Å). Due to the insertion of the water molecule, as shown in Figure 3b, the receptors were stacked in parallel and no longer cross-coupled as seen in Figure 1b. In addition, due to the interaction with water, the six-membered ring planes formed by the intramolecular hydrogen bonds in the urea groups on both sides of **L1** are closer to the same plane of the pyridine ring, the dihedral angle of which is 0.98° and 0.40°, respectively (the structure of **L1** is same as **L1'**).

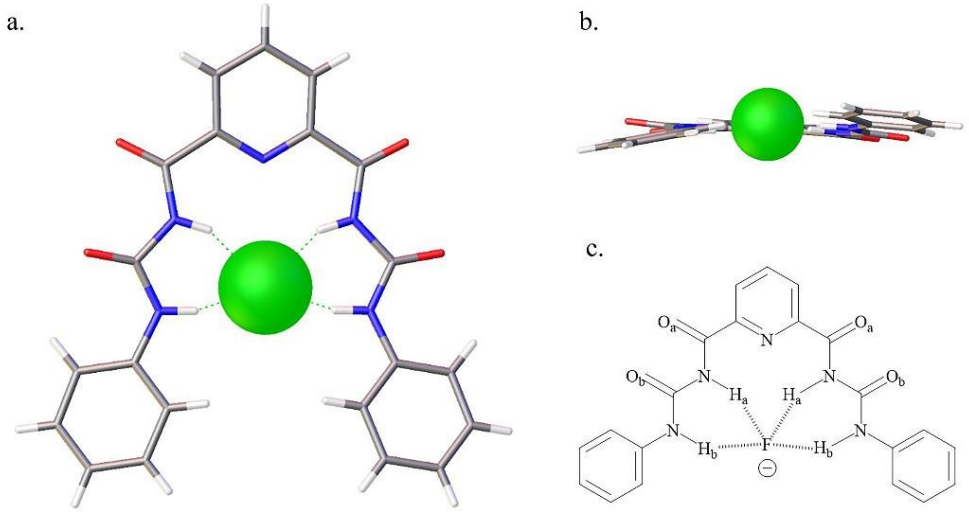

Figure 4. (a, b) Two views of the crystal structure of **L3·TBAF** (c) chemical structure of **L3·TBAF**. (TBA cation omitted for clarity; C: gray, H: white, O: red, N: blue, F: green)

The crystal structure of the **L3**·TBAF complex (TBAF: tetrabutylammonium fluoride) is shown in Figure 4a. The addition of an F^- ion destroys the two intramolecular hydrogen bonds (C=O_a···H_b–N), and the two single bonds (H_aN–CO_b) in the receptor are rotated, meaning that the conformations of the urea groups in **L3** are converted from a *trans* to a *cis* conformation. As a result, all of the four N–H groups can cooperatively surround the single F^- ion, forming four hydrogen bonds (1.792, 1.806, 1.966, and 1.973 Å). The receptor molecule is almost in the same plane as the F^- ion (Figure 4b). DFT calculations below will explore the differences between the *trans* and *cis* conformational stability of the receptor, and the change in the energy barriers for conformational transitions caused by F^- ions.

View Article Online
DOI: 10.1039/C9NJ05785D

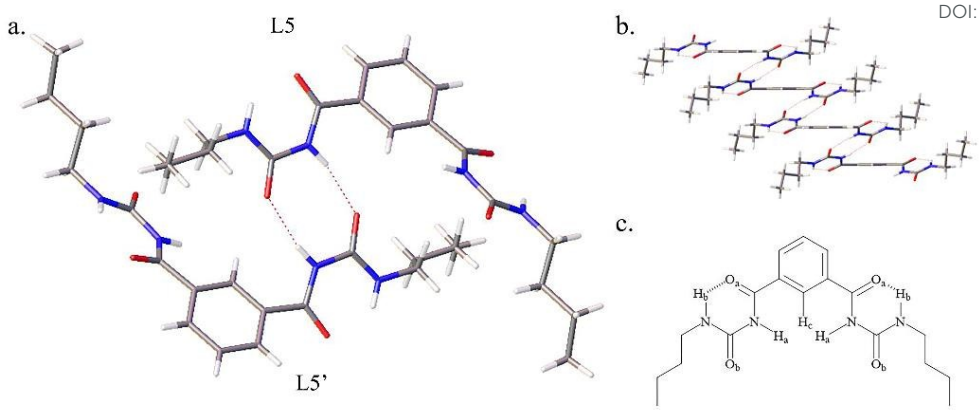

Figure 5. (a, b) Two views of the crystal structure of **L5** (c) chemical structure of **L5**. (C: gray, H: white, O: red, N: blue)

The crystal structure of **L5** is shown in Figure 5a. Similar to **L1-L3**, the carbonyl oxygen atoms (C=O_a) form intramolecular hydrogen bonds with the H_b–N on the adjacent urea group (C=O_a···H_b–N: 2.056, 2.056 Å). As shown in Figure 5b, the phenyl bisurea receptor **L5** differs from the pyridine bisurea receptors **L1-L3** in two ways. The first is that in **L5**, the C=O_b and N–H_a groups on one side form single intermolecular hydrogen bonds (2.048, 2.048 Å) with the N–H_a and C=O_b groups on one side of another molecule, and so the molecules take on a stacked configuration, rather than cross-linked as in **L1**. The second is that because of the small distances between N–H_a on both sides of the molecule and the H_c on the central benzene ring (2.085, 2.085 Å), these atoms mutually repel. This results in the six-membered ring planes formed by hydrogen bonding involving the carbonyl urea on both sides no longer being coplanar with the benzene ring, the dihedral angles being 27.2° and -27.2° (the structure of **L5** is same as **L5'**). One effect of this is that the volume of the cavity between the urea groups on both sides of **L5** (H_a to $H_{a'}$ distance: 3.996 Å) is larger than that of **L1** (H_a to $H_{a'}$ distance: 2.970 Å), **L2** (H_a to $H_{a'}$ distance: 2.842 Å) and **L3** (H_a to $H_{a'}$ distance: 2.992 Å). This may explain why the phenyl bisurea receptors have stronger affinity with larger volume anions such as HSO_4^- (28.7 $Å^3$) and Cl^- (24.8 $Å^3$)[61], while the binding ability of pyridine bisurea receptors with large anions is much weaker.

NMR titration

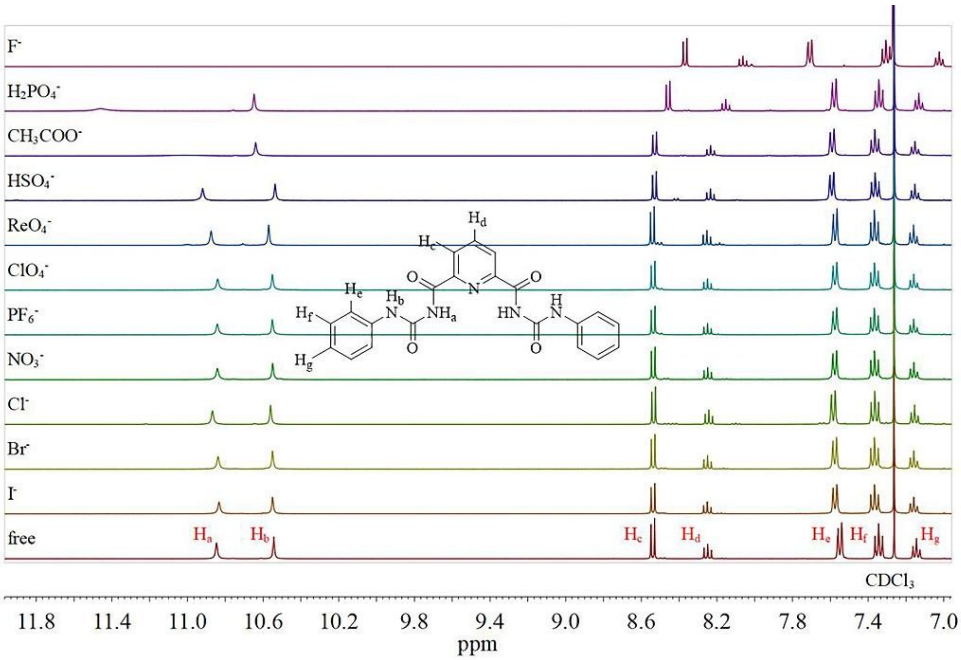

Figure 6. ^{1}H NMR spectra of **L3** (5 mM) with 1 equivalent of TBAx (where x is the anion shown in the figure) in $CDCl_3$ at 298 K.

In order to study the binding properties of the two types of receptors with anions, **L3** and **L4** were selected as being representative of the two types, and an NMR titration study was carried out. As shown in Figure 6, the addition of F^- ions leads to the disappearance of two peaks of the **L3** urea groups (H_a, H_b), indicating that F^- ion interacts strongly with four total N–H groups, suggesting that **L3** is likely to bind with F^- ions in a *cis-cis* conformation in solution. At the same time, the signals of the pyridine hydrogen atoms (H_c, H_d) move to higher field ($\Delta\delta$ 0.19, 0.17 ppm). The hydrogen signals of the benzene ring ($H_{e\text{-}g}$) appear to be slightly perturbed. Specifically, the signals from H_e and H_f move to higher field ($\Delta\delta$ 0.12, 0.04 ppm) while the signal from H_g moves to lower field ($\Delta\delta$ 0.16 ppm).

$H_2PO_4^-$ and CH_3COO^- only broaden one hydrogen signal of the urea group (H_a), and the shift in the signals from pyridine (H_c and H_d) shift by a smaller amount compared to the F^- case. The signals associated with the benzene ring ($H_{e\text{-}g}$) show no significant shift, indicating that **L3** interacts with $H_2PO_4^-$ and CH_3COO^- in a *trans-trans* conformation. The other anions induce almost no change in the chemical shifts of the **L3** hydrogen atoms, implying that these anions interact weakly with **L3**. In summary, the strength of the interaction between **L3** and this group of anions is consistent with the Hofmeister series.[62]

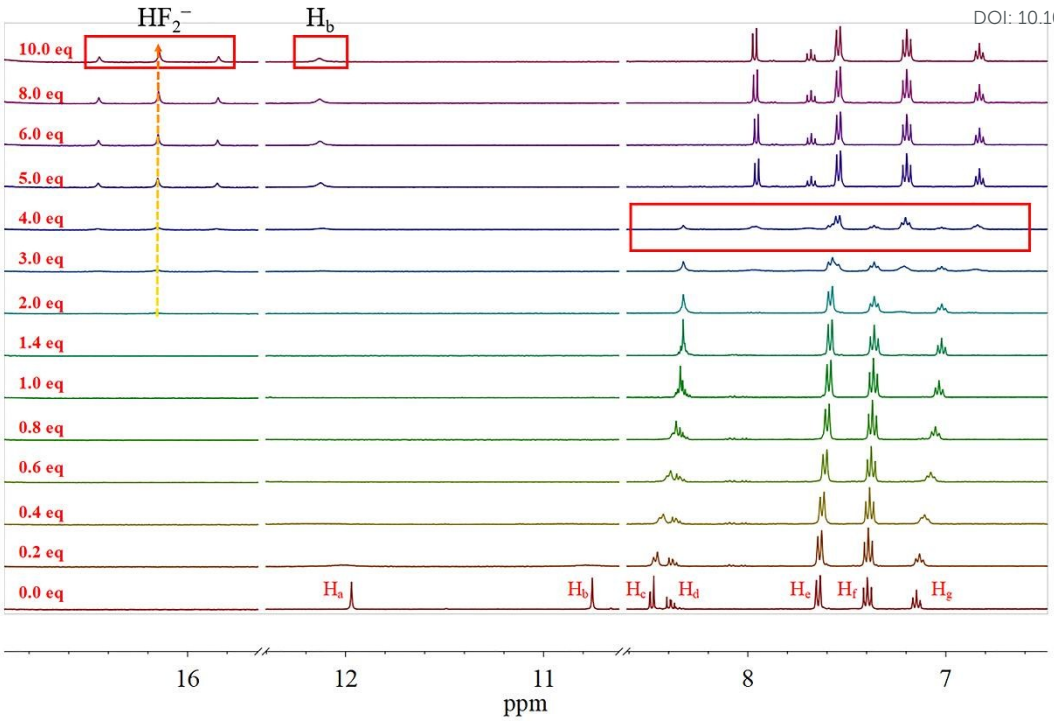

Figure 7. Stacked ^{1}H NMR spectra for titration of **L3** (0.002 M) with TBAF (0-10 equivalents) in DMSO-d_6 at 298 K.

The addition of one equivalent of F^- ions causes the disappearance of four NH groups hydrogen signals (Figure 6), which might be due to the strong interaction of intermolecular hydrogen bonds between F^- ions and NH groups, or the deprotonation of NH protons by F^- ions. To elucidate this, NMR titrations for **L3** with OH^- and F^- ions were carried out (Figure S7 and S8). Obviously, the addition of 0.5 equivalent of F^- ions leads to the disappearance of two peaks of the **L3** urea groups (H_a, H_b). In contrast, even the addition of OH^- ions up to 1.0 equivalent only leads to subtle shifts of the two peaks H_a and H_b. Moreover, at the same time, there are no HF_2^- signals appeared in the NMR spectrums (Figure 7), implying the abstraction of protons does not occur. These results reveal that the strong interaction between F^- ions and receptor **L3** causes the disappearance of NH proton signals. However, when two equivalent F^- ions are added, the deprotonation of NH_a group occurs. Specifically, the proton signal of the HF_2^- appears at around 16 ppm (Figure 7) and ^{19}F signal appears at −142 ppm (Figure S9). It is worth noting that the H_b signal reappears when 4 equivalent of F^- ions is added. We speculate that this may be due to the complete deprotonation of both N-H_a groups, resulting in the formation of the new anionic species $\mathbf{L3}^{2-}$.

As shown in Figure 8, the addition of F^- ions causes one hydrogen signal from the urea group of **L4,** H_a, to disappear, while the other hydrogen signal of the urea group, H_b, broadens and shifts slightly to lower field (Δδ 0.08 ppm). Meanwhile, one hydrogen signal from the benzene ring, H_c, shifts to lower field (Δδ 0.41 ppm), and two other hydrogen signals from the benzene ring, H_e and H_d, shift to high field (Δδ 0.03, 0.07 ppm).

The addition of $H_2PO_4^-$ or CH_3COO^- significantly shifts one hydrogen signal of the urea group of **L4,** H_a. F^- and $H_2PO_4^-$ have a strong interaction with the H_c on the benzene ring of **L4**, causing a change in the relative positions of the H_c and H_b signals. However, CH_3COO^- has little interaction with H_c. The addition of HSO_4^- or Cl^- can significantly shift one hydrogen signal of the urea group of **L4** (H_a). However, the other anions cause little change in the signal from this hydrogen.

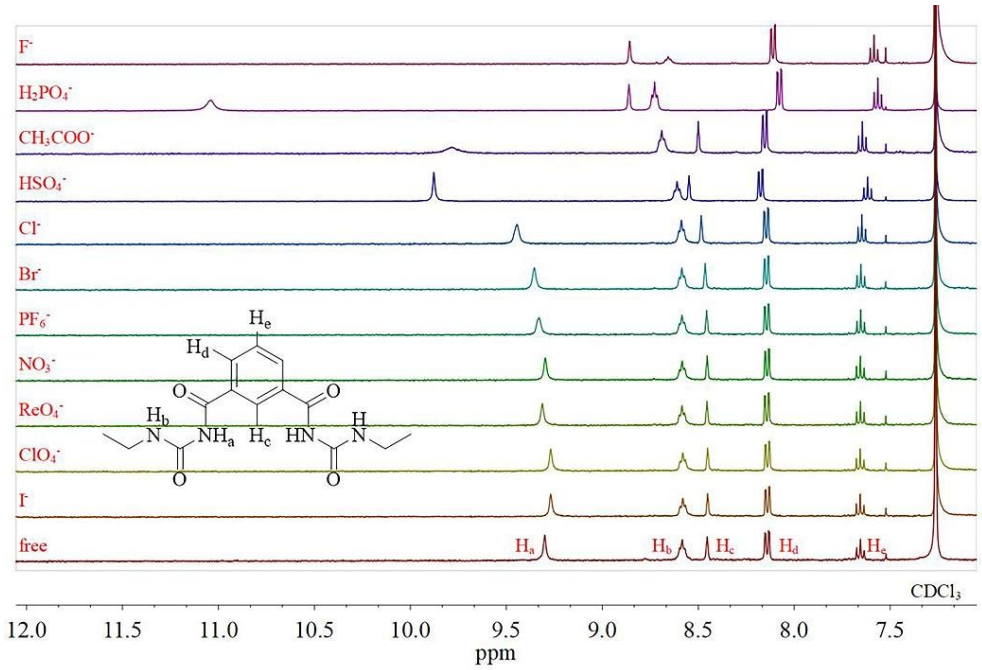

Figure 8. ^1H NMR spectra of **L4** (5 mM) with 1 equivalent of TBAx (where x is the anion shown in the figure) in $CDCl_3$ at 298 K.

These results indicate that although **L4** has a strong interaction with F^- ions, its binding mode is likely to be dominated by a *trans-trans* conformation, because the H_b signal of **L4** changes little, while both the H_a and H_b signals of **L3** completely disappear. Similarly, the binding mode of **L4** to $H_2PO_4^-$, CH_3COO^-, HSO_4^-, or Cl^- anions is likely to be in a *trans-trans* conformation. This finding is consistent with the result of the DFT calculations below. Note that the interaction between the two types of receptors and anions is slightly different. For example, HSO_4^- and Cl^- have a strong affinity with **L4**,

and a weak affinity with **L3**. This phenomenon might be due to matching of the receptor cavity size and the anion volume based on the analysis of crystal structure data.

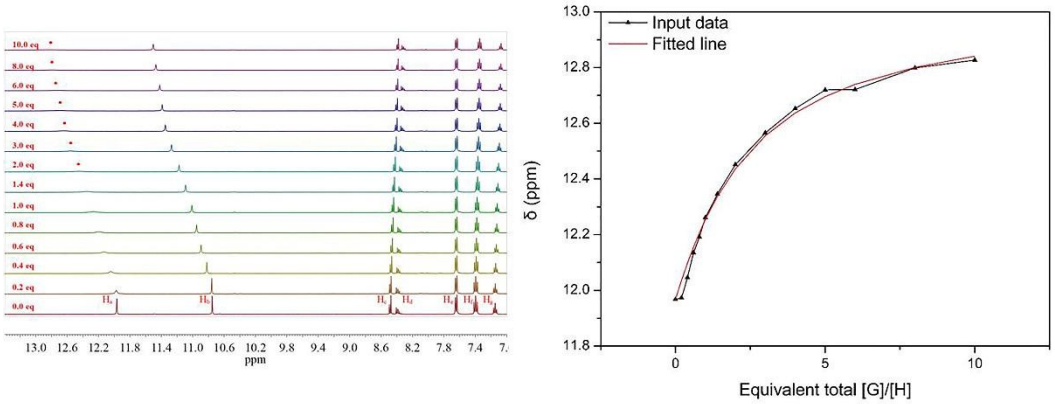

Figure 9. Stacked ^{1}H NMR spectra for titration of **L3** (0.002 M) with TBACH_3COO (0-10 equivalents) in DMSO-d_6 at 298 K (left), and chemical shifts of H_a protons of the **L3** plotted against the CH_3COO^- concentration (right).

Table 1. Association constants of anions with receptors **L3** and **L4**.[a]

Anion	L3	L4
CH_3COO^-	254	106
$H_2PO_4^-$	201	294

a: NMR titration, solvent: DMSO-d_6, 298 K, [L] = 2×10^{-3} M, anions added as TBA salts, where [TBAX] ~2×10^{-2} M; Models: 1:1; M^{-1}, errors <10%.

To verify this hypothesis, and to further understand the interactions between anions and the two types of receptors, we performed NMR titration experiments using **L3** and **L4** with varying concentrations of $H_2PO_4^-$ and CH_3COO^-. As an example, the left panel of Figure 9 shows the results of the titration of **L3** with CH_3COO^-. As the CH_3COO^- concentration increases gradually, the signals from H_a and H_b move toward lower field, while signals from H_c and H_d move to higher field. The chemical shifts of the H_a proton are fit to a curve (Figure 9, right), from which binding constants can be extracted, with a summary of results shown in Table 1.[63-65] The binding constant of **L3** with CH_3COO^- is slightly larger than that for $H_2PO_4^-$, which is consistent with the Hofmeister series. However, the binding constant of **L4** to $H_2PO_4^-$ is almost three times that of CH_3COO^-. This phenomenon is consistent with a larger cavity between the urea groups of the receptor, providing better spatial matching with large volume anions, so that the binding with $H_2PO_4^-$ is stronger ($H_2PO_4^-$ volume: 33.5 Å^3, CH_3COO^- volume: 17.8 Å^3).[61]

Theoretical studies

Table 2. Calculated binding energies for the receptor **L1** with three anions (kJ/mol).

Binding Energy	F^-	Cl^-	Br^-
cis-cis	−396.0	−254.5	−218.8
trans-trans	−269.2	−113.4	−87.4

To further explore the binding mechanism between urea receptors and anions, DFT calculations were performed on the receptor and receptor/anion complexes. First, the change in energy (ΔE) of the receptor **L1** in combination with several anions (F^-, Cl^-, Br^-) in the *cis-cis* and *trans-trans* conformations was compared, as shown in Table 2. The binding strength trend is $F^- > Cl^- > Br^-$, whether the receptor is in the *trans-trans* or *cis-cis* conformation. The DFT optimized structures of **L1** in *cis-cis* conformations with halide ions is shown in Figure 10. We found that when the *cis-cis* conformation of **L1** is combined with one F^- ion, it can be accommodated in the cavity of the four urea group NH, and the F^- ion and the pyridine ring are in the same plane. However, the combination of **L1** with other halide ions is different. For example, when a Cl^- ion is bound to four NH groups, it is out of the plane of the pyridine ring. The reason may be that due to the large volume of the Cl^- ion (F^- volume: 9.9 $Å^3$; Cl^- volume: 24.8 $Å^3$)[61], there is a poor match with the volume of the cavity formed by the four NH groups in **L1**. Further, the Br^- ion is farther away from the plane of the urea group and the pyridine ring, perhaps because of the even larger radius of the Br^- ion (Br^- volume: 31.5 $Å^3$)[61]. This result is consistent with the binding constants of **L3** with Cl^- ions (binding constant: 0.06) and Br^- ions (binding constant: 0.04) (Table S7), indicating much weaker interactions in comparison with pyridine receptor and F^- ion. Therefore, we suspect that pyridine bisurea receptors binds mainly to the F^- ion in a *cis-cis* conformation and a *trans-trans* conformation to larger volume anions such as Cl^- and Br^-. These findings are consistent with crystal structure analysis and the results of NMR titration.

View Article Online
DOI: 10.1039/C9NJ05785D

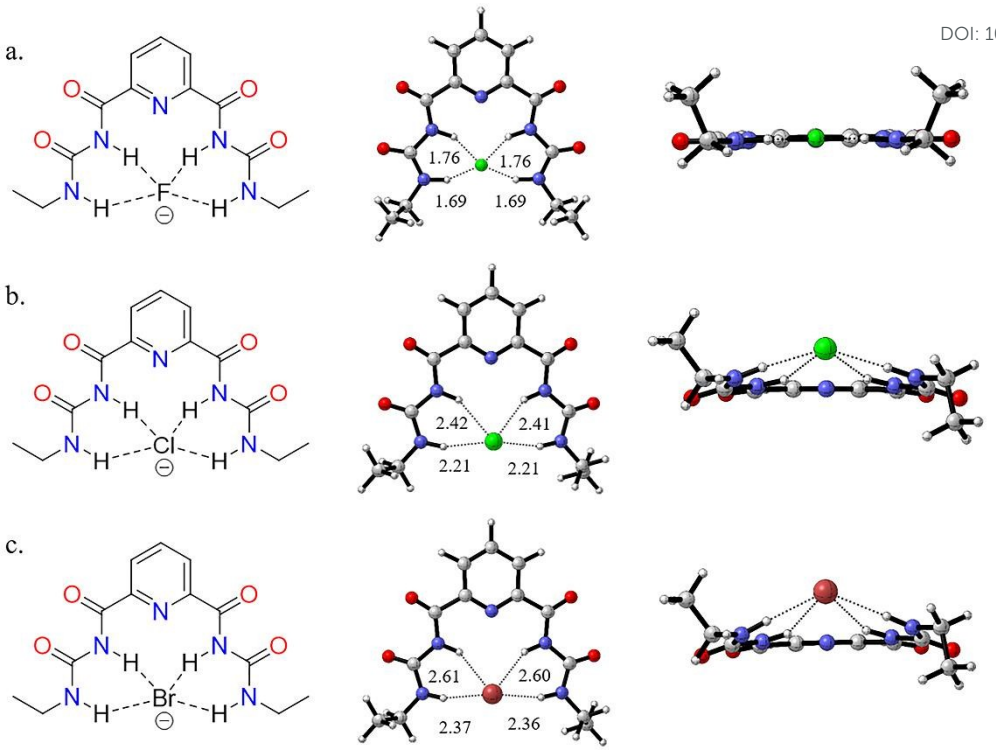

Figure 10. Optimized structures of **L1** with F^-(a), Cl^-(b), Br^-(c) anions in a *cis-cis* conformation at the M06-2X/6-311G(d,p) level.

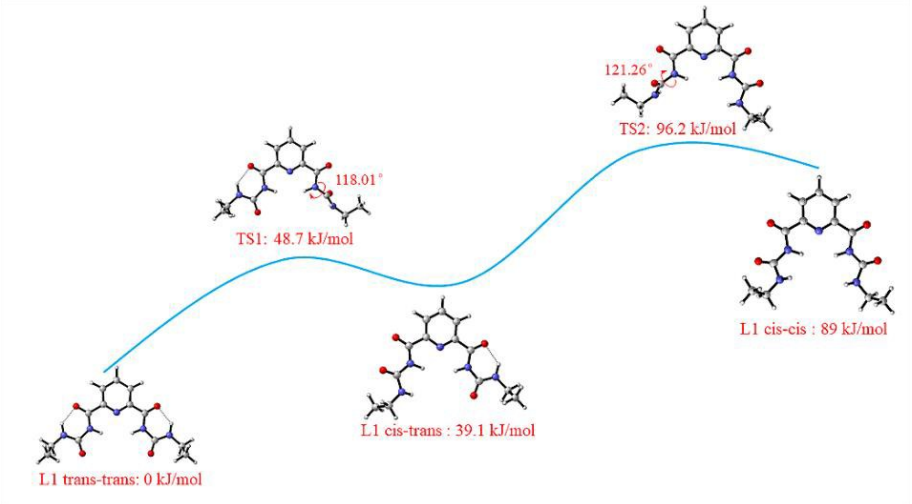

Figure 11. Energy profile for $(H_aN)-(CO_b)$ single bond rotation in **L1** at the M06-2X/def2TZVP level.

View Article Online
DOI: 10.1039/C9NJ05785D

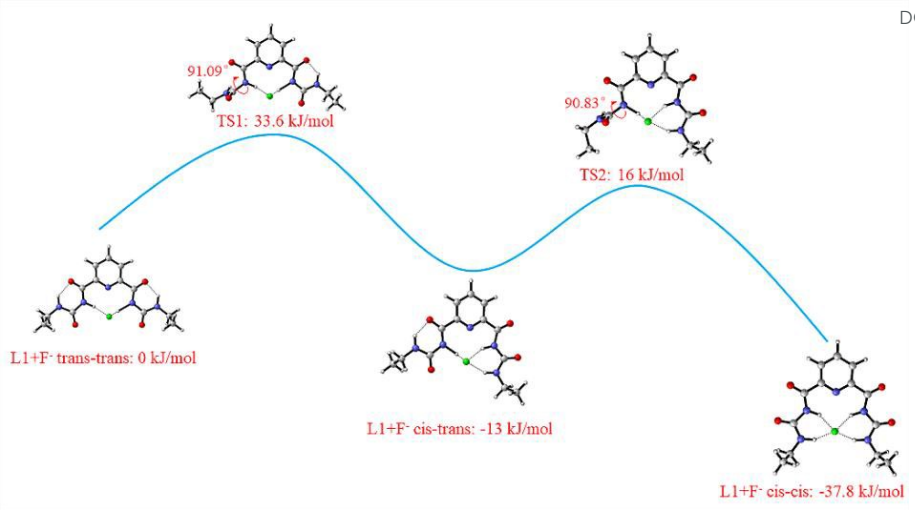

Figure 12. Energy profile for $(H_aN)-(CO_b)$ single bond rotation in **L1** bound to an F^- ion at M06-2X/def2TZVP level.

The discussion above has established that the receptor **L1** binds to the F^- ion in a *cis-cis* conformation, but it is not clear how the receptor undergoes conformational transitions in the presence of F^- ion. Therefore, conformational changes of the pyridine bisurea receptor and the receptor/F^- complex were studied using DFT calculations. It was found that, in the absence of F^- ions, **L1** can be transformed from a *trans-trans* to a *cis-cis* conformation by two $N-C(O_b)$ single bond rotations, as shown in Figure 11. However, this transformation is very difficult. Specifically, the energy barrier for a urea group to go from *trans* to *cis* is 48.7 kJ/mol, and the total energy barrier for both urea groups to go from *trans* to *cis* is 96.2 kJ/mol. Furthermore, due to the presence of two intramolecular hydrogen bonds, the *trans-trans* conformation of **L1** is more stable than the *cis-cis* conformation, with the *trans-trans* conformational energy being 89 kJ/mol lower. In contrast, when an F^- ion is present, the energy barriers for the two steps required for **L1** to go from *trans-trans* to *cis-cis* conformation are significantly reduced, as shown in Figure 12, to 33.6 kJ/mol and 29 kJ/mol. The relative energy of the receptor/F^- complex in a *cis-cis* conformation is 37.8 kJ/mol lower than that in a *trans-trans* conformation. This indicates that the F^- ion can promote an inversion in the conformation of the urea groups of **L1**, stabilize an intermediate *trans-cis* conformation, and further stabilize a *cis-cis* product conformation. These results are consistent with the crystal structure analysis discussed above.

View Article Online
DOI: 10.1039/C9NJ05785D

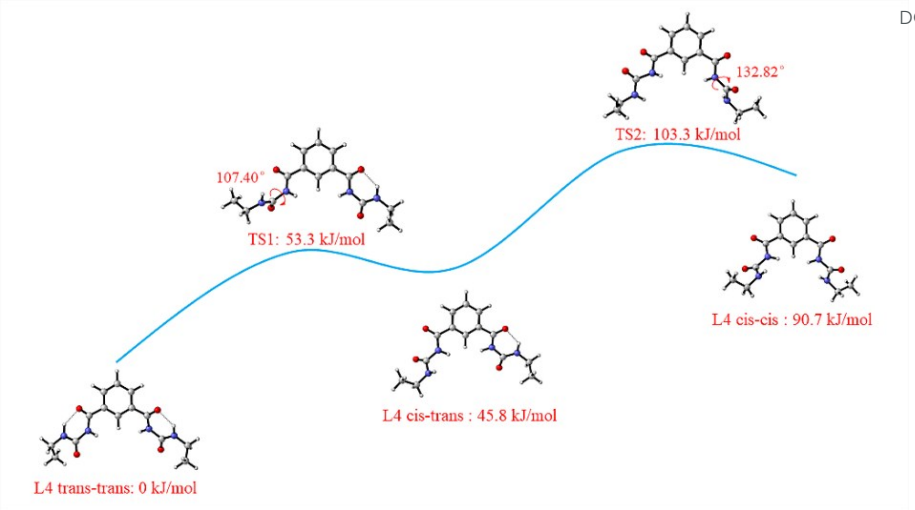

Figure 13. Energy profile for (H_aN)−(CO_b) single bond rotation in **L4** at the M06-2X/def2TZVP level.

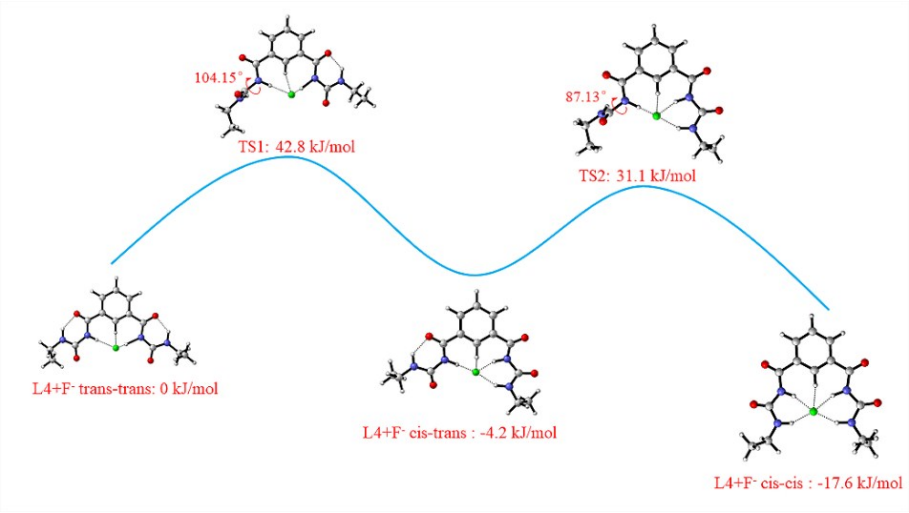

Figure 14. Energy profile for (H_aN)−(CO_b) single bond rotation in **L4** bound to an F^- ion at the M06-2X/def2TZVP level.

As a comparison with the pyridine ligands, we also calculated the energy profile for *trans-trans* to *cis-cis* conformational changes in the phenyl receptor **L4**. As shown in Figure 13, in the absence of F^- ion, it is also very difficult for **L4** to reconfigure to a *cis-cis* conformation from the *trans-trans* conformation, which requires two rotations of the (H_aN)−(CO_b)single bond. Specifically, the energy barrier for one of the urea groups to go from *trans* to *cis* is 53.3 kJ/mol, and the total energy barrier for the transition of both urea groups is 103.3 kJ/mol. In addition, similar to **L1**, **L4** is more stable in the *trans-trans* conformation compared to the *cis-cis* conformation due to the presence of two intramolecular hydrogen bonds, with the energy of the *trans-trans*

conformation 90.7 kJ/mol lower. As shown in Figure 14, when an F^- ion is present, the energy barriers for the urea group of **L4** to go from *trans-trans* to *cis-cis* are reduced to 42.8 and 35.3 kJ/mol. Also similar to **L1**, the receptor/F^- complex is more stable in the *cis-cis* conformation than the *trans-trans*, with the *cis-cis* energy 17.6 kJ/mol lower. By comparing the urea group transition processes of **L1** and **L4** (Figure 15), we find that the urea group conformational conversion energy barriers for **L4** are higher than that of **L1**, regardless of the presence of an F^- ion. In general, receptor **L1** is more likely to bind with an F^- ion in the *cis-cis* conformation.

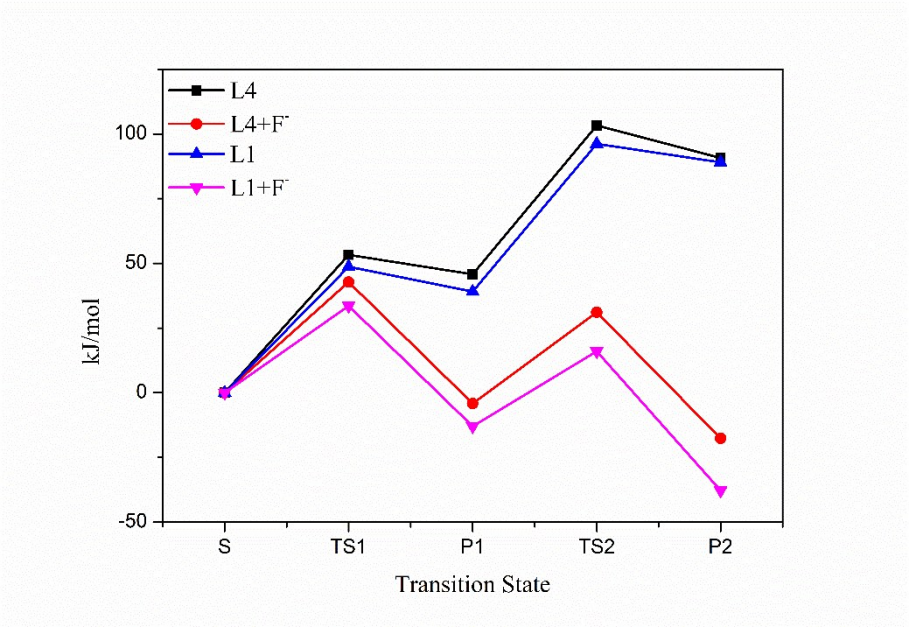

Figure 15. Energy profiles for $(H_aN)-(CO_b)$ single bond rotation at the M06-2X/def2TZVP level.

Conclusions

Two types of similar receptors, **L1-L5**, were synthesized and characterized. Crystal structure analysis indicated that the carbonyl group in these receptors participates in an intramolecular hydrogen bond with the N–H at the distal end of the urea group, forming a six-membered ring. This makes the *trans-trans* conformation more stable than the *cis-cis* conformation. The N_{py} atom of the pyridine receptors (**L1-L3**) forms two intramolecular hydrogen bonds with the proximal N–H of the urea groups, which promotes co-planarity of the two urea groups in the molecule. This reduces the volume of the cavity between the two urea groups, improving spatial matching to the small volume of the F^- ion. In contrast, the center C–H on the phenyl ring of the phenyl receptors (H_c in **L4** and **L5**) and the hydrogen atoms on the urea

groups of the two sides of the molecule have a mutual repulsion, enlarging the cavity of the two urea groups. The phenyl receptors favor binding larger volume anions. NMR titration studies further showed that although both types of receptors have strong affinities with the F^- ion, pyridine receptors have stronger affinity and higher selectivity for this ion. It was found by DFT that the pyridine receptor **L1** provides better spatial matching for the F^- ion. Both pyridine and phenyl based receptors are more stable in the *trans-trans* compared to *cis-cis* conformation. Binding to an F^- ion lowers the energy barrier for conformational change, and the receptor/F^- complex in *cis-cis* conformation is more stable compared to *trans-trans*. These results may provide a theoretical framework for selective detection of F^- ions, as well as the study of conformational stability and transformations in urea-based receptors.

Conflicts of interest

There are no conflicts to declare.

Acknowledgements

This work was supported by the National Natural Science Foundation of China (grant number: 21501123) and the International Collaboration Project of Department of Science and Technology of Sichuan Province, China (grant number: 2018HH0063). We would like to acknowledge the "Comprehensive Training Platform of Specialized Laboratory, College of Chemistry, Sichuan University" for HRMS, NMR and XRD analyses. We appreciate the help from Dr. Yue Qi and Dr. Meng Yang for X-ray diffraction measurements of single-crystal.

View Article Online
DOI: 10.1039/C9NJ05785D

Reference

1 J. L. Sessler, P. A. Gale and W.-S. Cho, *Anion Receptor Chemistry: Monographs in Supramolecular Chemistry*, RSC, Cambridge, UK, 2006.
2 S. O. Kang, R. A. Begum and K. Bowman-James, *Angew. Chem. Int. Ed.*, 2006, **45**, 7882–7894.
3 J. R. Hume, D. Duan, M. L. Collier, J. Yamazaki and B. Horowitz, *Physiol Rev.*, 2000, **80**, 31–81.
4 M. S. Vickers and P. D. Beer, *Chem. Soc. Rev.*, 2007, **36**, 211– 225.
5 R. G. Van Kesteren, S. A. Duursma, W. J. Visser, V. Van der Sluys and O. Backer Dicks, *Metab. Bone Dis. Rel. Res.*, 1982, **4**, 31–37.
6 C. I. Lin, S. Selvi, J. M. Fang, P. T. Chou, C. H. Lai and Y. M. Cheng, *J. Org. Chem.*, 2007, **72**, 3537–3542.
7 K. Müller, C. Faeh and F. Diederich, *Science*, 2007, **317**, 1881–1886.
8 Stockbridge R. B., Robertson J. L., Kolmakova-Partensky L. and Miller C., *Elife*, 2013, **2**, e01084.
9 Ozsvath D. L., *Rev. Environ. Sci. Biotechnol.*, 2008, **8**, 59–79.
10 Kaminsky L. S., Mahoney M. C., Leach J., Melius J. and Miller M. J., *Crit. Rev. Oral. Biol. Med.*, 1990, **1**, 261–281.
11 Ai-Fang Li, Jin-He Wang, Fang Wang and Yun-Bao Jiang, *Chem. Soc. Rev.*, 2010, **39**, 3729–3745.
12 V. Amendola, L. Fabbrizzi and L. Mosca, *Chem. Soc. Rev.*, 2010, **39**, 3889–3915.
13 V.B. Bregovic, N. Basaric and K. Mlinaric-Majerski, *Coordin Chem Rev.*, 2015, **295**, 80–124.
14 S.-Y. Liu, Y.-B. He, J.-L. Wu, L.-H. Wei, H.-J. Qin, L.-Z. Meng and L. Hu, *Org. Biomol. Chem.*, 2004, **2**, 1582-1586.
15 J. Scheerder, J.P.M. van Duynhoven, J.F.J. Engbersen and D.N. Reinhoudt, *Angew. Chem. Int. Ed.*, 1996, **35**, 1090–1093.
16 J.N. Babu, V. Bhalla, M. Kumar, R.K. Mahajan and R.K. Puri, *Tetrahedron Lett.*, 2008, **49**, 2772–2775.
17 S. O. Kang and K. C. Nam, *Bull. Korean Chem. Soc.*, 2002, **23**, 640–642.
18 P. Tongraung, N. Chantarasiri, and T. Tuntulani, *Tetrahedron Lett.*, 2003, **44**, 29–32.
19 Á. Lorenzo, E. Aller and P. Molina, *Tetrahedron*, 2009, **65**, 1397–1401.
20 Pratt M. D. and Beer P. D., *Polyhedron*, 2003, **22**, 649–653.
21 Xie H. Z., Yi S., Yang X. P. and Wu S. K., *New J. Chem.*, 1999, **23**, 1105–1110.
22 Berrocal M. J., Cruz A., Badr I. H. A. and Bachas L. G., *Anal. Chem.*, 2000, **72**, 5295–5299.
23 Va´clav Stastny, Pavel Lhota´k, Veronika Michlova´, Ivan Stibor and Jan Sykora, *Tetrahedron*, 2002, **58**, 7207–7211.
24 Denys Meshcheryakov, Michael Bolte and Volker Böhmer, *Tetrahedron Lett.*, 2010, **51**, 1202–1204.
25 Jeffrey M. Engle, Pushpinder S. Singh, Chris L. Vonnegut, Lev N. Zakharov, Darren W. Johnson and Michael M. Haley, *CrystEngComm*., 2014, **16**, 3703 – 3706.
26 Liguo Ji, Zaiwen Yang, Yanxia Zhao, Meng Sun, Liping Cao, Xiao-Juan Yang, Yao-Yu Wang and Biao Wu, *Chem. Commun*., 2016, **52**, 7310—7313.
27 M. Barboiu, G. Vaughan and A. van der Lee, *Org. Lett.*, 2013, **5**, 3073−3076.
28 J.H. Lee, J.H. Lee, Y.R. Choi, P. Kang, M.-G. Choi and K.-S. Jeong, *J. Org. Chem.*, 2014, **79**, 6403−6409.
29 G. Sanchez, A. Espinosa, D. Curiel, A. Tarraga and P. Molina, *J. Org. Chem.*, 2013, **78**, 9725−9737.
30 S.K. Kim and J. Yoon, *Chem. Commun.*, 2002, **7**, 770−771.
31 S.K. Kim, N.J. Singh, S.J. Kim, K.M.K. Swamy, S.H. Kim, K.-H. Lee, K.S. Kim and J. Yoon, *Tetrahedron*, 2005, **61**, 4545−4550.
32 Vyacheslav S. Bryantsev, Timothy K. Firman and Benjamin P. Hay, *J. Phys. Chem. A.*, 2005, **109**, 832−842.
33 Rafilovich M., Bernstein J., Harris R. K., Apperley D. C., Karamertzanis P. G. and Price S. L., *Cryst. Growth Des.*, 2005, **5**, 2197− 2209.
34 Etter M. C., Urbanczyk-Lipkowska Z., Zia-Ebrahimi M. and Panunto T. W., *J. Am. Chem. Soc.*, 1990, **112**, 8415−8426.
35 Huang K.-S., Britton D., Etter M. C. and Byrn S. R., *J. Mater. Chem.*, 1995, **5**, 379−383.
36 Lappert M. F., Alvarez S., Aullon G., Fandos R., Otero A., Rodriguez A., Rojas S. and Terreros P., *Eur. J. Inorg. Chem.*, 2009, **13**, 1851−1860.
37 DeSouza W. F., Kambe N., Jin Z. J., Kanehisa N., Kai Y. and Sonoda N., *J. Org. Chem.*, 1995, **60**, 7058−7062.
38 G. M. Whitesides, J. P. Mathias and C. T. Seto, *Science*, 1991, **254**, 1312–1319.
39 Y. Kervella, E. Shilova, S. Latil, B. Jousselme and F. Silly, *Langmuir*, 2015, **31**, 13420–13425.
40 D. Reisser, and J.F. Jeannin, *Adv. Exp. Med. Biol.*, 2009, **667**, 101–110.
41 Nithi Phukan and Jubaraj B. Baruah, *ChemistrySelect.*, 2016, **3**, 440–443
42 J. A. Theobald, N. S. Oxtoby, M. A. Phillips, N. R. Champness and P. H. Beton, *Nature*, 2003, **424**, 1029–1031.
43 W. Xu, R. E. A. Kelly, H. Gersen, E. Lagsgaard, I. Stensgaard, L. N. Kantorovich, F. Besenbacher, *Small*, 2009, **5**, 1952–1956.
44 D. L. Keeling, N. S. Oxtoby, C. Wilson, M. J. Humphry, N. R. Champness and P. H. Beton, *Nano Lett.*, 2003, **3**, 9–12.
45 M. Stohr, M. Wahl, C. H. Galka, T. Riehm, T. A. Jung and L. H. Gade, *Angew. Chem., Int. Ed.*, 2005, **44**, 7394–7398.
46 J. P. Rabe and S. Buchholz, *Science*, 1991, **253**, 424–427.
47 T. Yokoyama, S. Yokoyama, T. Kamikado, Y. Okuno and S. Mashiko, *Nature*, 2001, **413**, 619–621.
48 Xi Shu, Ruyu Wang, Yu Fan, Shoujian Li and Chao Huang, *Tetrahedron Lett.*, 2019, **60**, 729–733.
49 Ruyu Wang, Xi Shu, Yu Fan, Shoujian Li, Yongdong Jin and Chao Huang, *RSC Adv.*, 2018, **8**, 39394-39407.

50 Damjan Makuc, Jennifer R. Hiscock, Mark E. Light, Philip A. Gale and Janez Plavec, *Beilstein J. Org. Chem.*, 2011, **7**, 1205–1214.
51 Damjan Makuc, Markus Albrecht and Janez Plavec, *Supramolecular Chemistry.*, 2010, **22**, 603–611.
52 Shofiur Rahman, Hirotsugu Tomiyasu, Hiroto Kawazoe, Jiang-Lin Zhao, Hang Cong, Xin-Long Ni, Xi Zeng, Mark R. J. Elsegood, Thomas G. Warwick, Simon J. Teat, Carl Redshaw, Paris E. Georghioub and Takehiko Yamato, *New J. Chem.*, 2016, **40**, 9245—9251.
53 Hayley A. Burkill, Neil Robertson, Ramo´n Vilar, Andrew J. P. White and David J. Williams, *Inorg. Chem.*, 2005, **44**, 3337−3346.
54 Dolomanov, O.V., Bourhis, L.J., Gildea, R.J, Howard, J.A.K. and Puschmann, H., *J. Appl. Cryst.*, 2009, **42**, 339-341.
55 Sheldrick, G.M., *Acta Cryst.*, 2008, **A64**, 112-122.
56 Sheldrick, G.M., *Acta Cryst.*, 2015, **C71**, 3-8.
57 M. J. Frisch, G. W. Trucks, H. B. Schlegel, G. E. Scuseria, M. A. Robb, J. R. Cheeseman, G. Scalmani, V. Barone, B. Mennucci, G. A. Petersson, H. Nakatsuji, M. Caricato, X. Li, H. P. Hratchian, A. F. Izmaylov, J. Bloino, G. Zheng, J. L. Sonnenberg, M. Hada, M. Ehara, K. Toyota, R. Fukuda, J. Hasegawa, M. Ishida, T. Nakajima, Y. Honda, O. Kitao, H. Nakai, T. Vreven, J. A. Montgomery Jr., J. E. Peralta, F. Ogliaro, M. Bearpark, J. J. Heyd, E. Brothers, K. N. Kudin, V. N. Staroverov, R. Kobayashi, J. Normand, K. Raghavachari, A. Rendell, J. C. Burant, S. S. Iyengar, J. Tomasi, M. Cossi, N. Rega, J. M. Millam, M. Klene, J. E. Knox, J. B. Cross, V. Bakken, C. Adamo, J. Jaramillo, R. Gomperts, R. E. Stratmann, O. Yazyev, A. J. Austin, R. Cammi, C. Pomelli, J. W. Ochterski, R. L. Martin, K. Morokuma, V. G. Zakrzewski, G. A. Voth, P. Salvador, J. J. Dannenberg, S. Dapprich, A. D. Daniels, Ö. Farkas, J. B. Foresman, J. V. Ortiz, J. Cioslowski, D. J. Fox, Gaussian 09, Revision D. 01, Gaussian Inc., Wallingford, CT, 2013.
58 Y. Zhao and D. G. Truhlar, *Theor. Chem. Acc.*, 2008, **120**, 215–241.
59 F. Weigend and R. Ahlrichs, Phys. *Chem. Chem. Phys.*, 2005, **7**, 3297–3305.
60 C. Y. Legault, CYLVIEW, 1.0b, Université de Sherbrooke, 2009; http://www.cylview.org.
61 Yizhak Marcus, H. Donald Brooke Jenkins and Leslie Glasser, *J. Chem. Soc., Dalton Trans.*, 2002, 3795-3798
62 Kajetan Dabrowa, Filip Ulatowski, Dawid Lichosyt and Janusz Jurczak, *Org. Biomol. Chem.*, 2017, **15**, 5927-5943.
63 P. Thordarson, *Chem. Soc. Rev.*, 2011, **40**, 1305-1323.
64 D. B. Hibbert and P. Thordarson, *Chem. Commun.*, 2016, **52**, 12792-12805.
65 E. N. W. Howe, M. Bhadbhade and P. Thordarson, *J. Am. Chem. Soc.*, 2014, **136**, 7505-7516.

View Article Online
DOI: 10.1039/C9NJ05785D

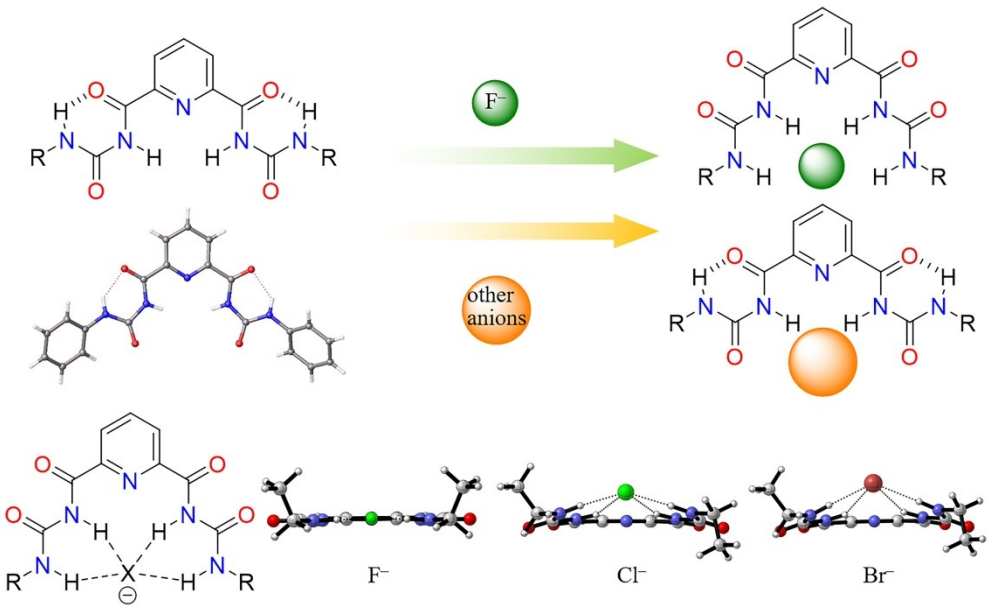

303x182mm (300 x 300 DPI)